Proceedings of the 20th International Conference on Soil Mechanics and Geotechnical Engineering– Rahman and Jaksa (Eds)

Seismic analysis of rock tunnels: a parametric analysis

Analyse sismique des tunnels de roche: une analyse paramétrique

Abdelwahhab N. Salem & Omar Y. Ezzeldine & Mohamed I. Amer
Soil Mechanics and Foundation, Faculty of Engineering, Cairo University, Giza, Egypt

ABSTRACT: Parametric analysis is conducted to study seismic behavior of different sizes of rock tunnels, constructed in different rock conditions, and subjected to the same seismic load. The initial stress condition for each case is quantified using three-dimensional finite element analyses. The seismic loading acts on the final lining as a long-term loading condition. Typical quasi-static seismic analysis is carried out along with full-scale seismic analysis approaches. Full-scale seismic analyses used real-time history motion of the Duzce 1999 earthquake and sinusoidal seismic wave. Results of full-scale analyses are compared to those of quasi-static analyses in terms of straining actions on tunnel final lining and of shear stress induced in the rock mass.

RÉSUMÉ : Une analyse paramétrique est effectuée pour étudier le comportement séismique de différentes tailles de tunnels rocheux, construits dans différentes conditions rocheuses et soumis à la même charge séismique. L'état de la contrainte initiale pour chaque cas est quantifié à l'aide d'analyses d'éléments finis tridimensionnels. La charge séismique agit sur le revêtement final comme condition de chargement à longue terme. L'analyse séismique quasi statique typique est comparée avec des approches d'analyse séismique à grande échelle. Les analyses séismiques à grande échelle sont basées sur l'historique de temps réel de mouvement de tremblement de terre de Duzce en 1999 et de l'onde séismique sinusoïdale. Les résultats des analyses à grande échelle sont comparés avec ceux de l'analyse quasi statique en termes d'actions de contrainte sur le revêtement final du tunnel et de la contrainte de cisaillement induit dans la masse rocheuse.

KEYWORDS: Seismic, Quasi-static, Full-scale, Rock, Tunnel.

1 INTRODUCTION.

Seismic effect on rock tunnels is studied in the transverse direction either through simple closed-form solution (Wang 1993; Penzien 2000) or through more elaborate numerical analyses. Numerical analyses are categorized as pseudo-static, quasi-static, and full-scale numerical analyses. Each category provides a certain degree of accuracy and complexity with the most accurate and complex category is the full-scale numerical analysis.

The pseudo-static analysis consists of inducing factored horizontal and vertical accelerations to the model domain to represent Peak Ground Acceleration PGA that can be derived from a separate one-dimensional, free-field site response analysis. In Quasi-static numerical analysis, the maximum shear strain of the ground in free-field condition as proposed by (Wang 1993, Power et al. 1998; Hashash et al. 2001), is imposed on the entire ground mass. Hence, straining actions acting in the final tunnel lining and stresses in the ground are obtained accordingly. This approach is applied by Pescara et al 2011. Full-scale seismic numerical analyses were applied through Finite Element Modeling F.E.M. or Finite Difference Modeling F.D.M. as described by (Joshi & Emery 1980, Sarfeld et al. 1985, Lee & An 2001, Corigliano et al. 2007, Bilotta et al. 2007 and Lanzano 2009). This analysis needs detailed input static and dynamic parameters and advanced constitutive models. Such parameters incorporate variation law of the stiffness G and damping ratio D_0 with the shear strain γ. The major advantage of this method is that it realistically represents the seismic loading either through real earthquake time history or through sinusoidal wave loading.

The quasi-static approach is the most widely used in seismic analysis because of its simplicity as it only uses static ground parameters. Nevertheless, the comparison between this approach and the other more realistic full-scale modeling is not sufficiently discussed in the literature.

One main reason why such comparison is rare in the literature is due to the fact that seismic loading is a long-term loading. The state of stress receptive to seismic loading should be quantified through elaborate three-dimensional analyses that model tunnel construction and the application of the primary lining.

Parametric analysis of seismic action on rock material is achieved through the following steps:

1. Considering different conditions of tunnel sizes and rock qualities, a matrix of cases of different tunnel sizes is considered with different rock qualities as described by Barton Q classification system (NGI 1997 and Barton et al. 1974).
2. Rock classification system mentioned above provides, for each case a scheme of preliminary lining system that is mostly different from the other cases.
3. For each case, the effect of tunnel excavation and application of primary lining is estimated through three-dimensional finite element modeling. This step allows for the estimation of the degree of stress relief around the excavated tunnel prior to the installation of the final lining.
4. Final lining, made of reinforced concrete, interacts with the ground stress condition reached through the previous step and is affected by long-term loading condition. This condition is mainly due to the deterioration of the primary lining system.
5. After the above steps are made, seismic action can be induced to allow for the study of straining actions on the final lining and of the seismic stresses in the ground mass.

In this paper, an attempt has been made to address the above aspects. In this vein, a series of numerical models have been developed using PLAXIS finite element modeling program for three tunnel sizes constructed using conventional tunneling with sprayed concrete lining (NATM) in three different rock quality medium. The numerical analyses performed considered the three-dimensional behavior, initial stress conditions, rock support system, construction sequence, static and dynamic rock parameters, and loading conditions (static, quasi-static, and full-scale seismic).

2 CASES OF TUNNELS UNDER STUDY.

Three tunnel sizes (17.4, 10, and 5m) were used in this study analyses to cover ranges of tunnel dimensions usually constructed in real life. The crown depth of tunnels was fixed to 29m to represent a case of a deep tunnel. The rock initial support configurations of tunnels were deduced from the rock

quality Q classification system (NGI 1997) that was first introduced by (Barton et al. 1974) and lately updated by (Grimstad 2007). Three Q-values (0.02, 0.4, and 4.0) were proposed for this study to cover a range of extremely poor to fair rock classes. A total of 9 tunnel configurations were developed for the three tunnel sizes and three rock Q-values as given in (Table 1). An example of rock initial support for tunnels with sizes 17.4, 10, and 5m constructed in rock quality Q=0.02 are given in (Figures 1, 2, and 3), respectively.

Table 1. Rock initial support Models of tunnel sizes 17.4, 10, and 5m in the three rock classes (Q=0.02, 0.4, and 4.0).

Model No.	Tunnel size D (m)	Q (RMR)	Primary Support System
1	17.4	Q=0.02 (RMR=25)	Fiber-reinforced Concrete 35cm thick + wire mesh + Systematic Y26 Bolt Length 6m and Spacing 1.5m + Steel Arch 2HEB-140 Spacing 2.6m.
4	10.0		Fiber-reinforced Concrete 35cm thick + wire mesh + Systematic Y26 Bolt Length 3m and Spacing 1.0m + Steel Arch HEB-140 Spacing 2.6m.
7	5.0		Fiber-reinforced Concrete 20cm thick + wire mesh + Systematic Y26 Bolt Length 2.4m and Spacing 1.0m + Steel Arch HEB-120 Spacing 2.6m.
2	17.4	Q=0.4 (RMR=44)	Fiber-reinforced Concrete 15cm thick + wire mesh + Systematic Y26 Bolt Length 6m and Spacing 2.0m + Steel Arch HEB-140 Spacing 4.0m.
5	10.0		Fiber-reinforced Concrete 12cm thick + wire mesh + Systematic Y26 Bolt Length 3m and Spacing 1.5m.
8	5.0		Fiber-reinforced Concrete 10cm thick + wire mesh + Systematic Y26 Bolt Length 2.4m and Spacing 1.5m.
3	17.4	Q=4.0 (RMR=59)	Fiber-reinforced Concrete 9cm thick + wire mesh + Systematic Y26 Bolt Length 6m and Spacing 2.5m.
6	10.0		Fiber-reinforced Concrete 6cm thick + wire mesh + Systematic Y26 Bolt Length 3m and Spacing 2.0m.
9	5.0		Fiber-reinforced Concrete 5cm thick + wire mesh + Systematic Y26 Bolt Length 2.4m and Spacing 2.0m.

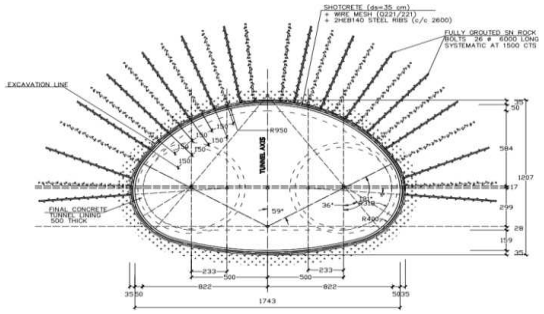

Figure 1. Initial rock support system of Model 1 (Q=0.02, D=17.4m).

3 TWO- AND TREE DIMENSIONAL ANALYSES

Tunneling causes changes in the three-dimensional stress-strain behavior in the ground. Convergence confinement method (β-method) is an approximation to account for the three-dimensional tunneling effects in the plane strain two-dimensional transverse model.

Due to delayed installation of the shotcrete lining convergence of the surrounding rock towards the cavity takes place, which results in a stress relaxation in the rock. The initial ground pressure p_0 on the tunnel is reduced to $[(1-\beta)^* p_0]$ with $0<\beta<1$ where β is the load reduction factor. In PLAXIS, this factor is expressed by the input value $\Sigma MStage$ where $\Sigma MStage=1-\beta$.

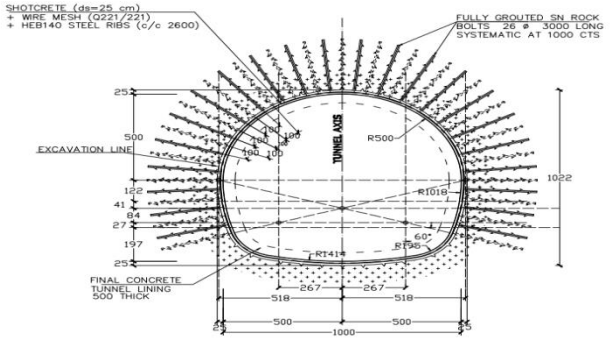

Figure 2. Initial rock support system of Model 4 (Q=0.02, D=10m).

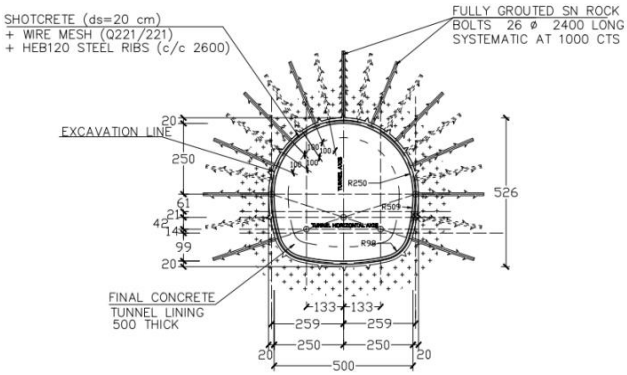

Figure 3. Initial rock support system of Model 7 (Q=0.02, D=5m).

3.1 *Material Parameters*

In the F.E. analysis, the primary support made of sprayed shotcrete is modeled using two different parameter sets for shotcrete; young and old. In the first calculation phase after excavation, the tunnel lining is activated with the material parameter set as shotcrete young. In the following phases, shotcrete parameters are set as old condition. The final lining material behavior is linear-elastic. The thickness of the final lining is taken 50.0 cm for all models. Lining properties are given in (Table 2). Damping ratio (ξ) is taken 3% for all cases.

Table 2. Lining Material Parameters.

Parameters	γ (kN/m^3)	E (MN/m^2)	ν (-)	ξ (%)
Shotcrete Young	25	4000	0.2	3
Shotcrete Old	25	15000	0.2	3
Concrete	25	30000	0.15	3

The load-bearing behavior of the systematic rock bolting is modeled as elastic embedded beams with parameters given in (Table 3).

Table 3. Rock Bolt Material Parameters.

Parameters		Value
E	(MN/m^2)	2.05E+05
γ	(kN/m^3)	78
Beam Type		Predefined
Predefined beam type		Massive Circular beam
Diameter	(m)	0.026
Axial skin resistance		Linear
$T_{skin,\,start,\,max}$	(kN/m)	126
$T_{skin,\,end,\,max}$	(kN/m)	126

The ground profile consists of a superficial 9.0 m fill layer followed by a rock layer 70.0 m thick with groundwater level at the ground surface. The input geotechnical parameters for

superficial man-made fill and alluvial fill are given in (Table 4). The input geotechnical parameters of rock assumed with three rock qualities are interpreted from Q-values (0.02, 0.4, and 4.0) as given in (Table 5). The E_{50} is the rock mass modulus E_{rm} calculated from (Hoek-Diederichs 2006) with the intact rock modulus E_i assumed by (Palmstrom and Singh 2001). Dynamic Modulus $E_{dynamic}$ is obtained using (Gutenberg 1951) equation by substituting with compression wave velocity corresponding to Q-value using the equation proposed by (Barton 2002) and shear wave velocity that obtained using (Stein and Wysession 2003). The rest of the parameters are obtained using equations in (Table 4). From the presented parameters, static parameters are used in quasi-static analysis while dynamic parameters are used in the full-scale seismic analyses.

Table 4. Geo-mechanical characteristics of the Superfacial fill layers.

Parameter			Fill
Unit Weight	γ	(kN/m^3)	19
Bulk Density	ρ	(kN/m^3)	1.94
Cohesion	c	(MPa)	0
Friction Angle	ϕ	(°)	23
Dilatancy Angle	ψ	(°)	0
At Rest Earth Pressure Coef.	K_o	(-)	0.61
Poisson's Ratio	ν	(-)	0.35
Unload/Reload Poisson's Ratio	ν_{ur}	(-)	0.20
Static Deformation Modulus	$E_{static} = E_{50}$	(MPa)	15
Static Shear Modulus	$G_{static} = E_{static}/2*(1+\nu)$	(MPa)	6
Quasi-static Def. Modulus	$E_{quasi\text{-}static} = E_{ur} = 2*E_{static}$	(MPa)	30
Quasi-static Shear Modulus	$G_{quasi\text{-}static} = E_{quasi\text{-}static}/2*(1+\nu_{ur})$	(MPa)	13
Quasi-static Shear Wave Velocity	$C_S = (G_{quasi\text{-}static}/\rho)^{0.5}$	(m/s)	80
Seismic Deformation Modulus	$E_{seismic} = E_d$	(MPa)	153
Seismic Shear Modulus	$G_{max} = G_o = E_d/2*(1+\nu_{ur})$	(MPa)	64
Shear Wave Velocity	$V_S = (G_{max}/\rho)^{0.5}$	(m/s)	181
Damping Ratio	ξ	(%)	3

Table 5. Interpreted Geo-mechanical characteristics of the three rock classes (Q=0.02, 0.4 and 4.0) used as input for models

Parameter		Q=0.02	Q=0.4	Q=4.0
γ	(kN/m^3)	25	25	25
ρ	(kN/m^3)	2.55	2.55	2.55
c	(MPa)	0.135	0.178	0.444
ϕ	(°)	32	42	51
ψ	(°)	0	0	0
K_o	(-)	0.470	0.331	0.223
ν	(-)	0.30	0.30	0.30
ν_{ur}	(-)	0.20	0.20	0.20
E_{static}	(MPa)	300	1000	6400
G_{static}	(MPa)	115	385	2462
$E_{quasi\text{-}static}$	(MPa)	600	2000	12800
$G_{quasi\text{-}static}$	(MPa)	250	833	5333
C_S	(m/s)	313	572	1447
$E_{seismic}$	(MPa)	6638	19618	34306
G_{max}	(MPa)	2765.9	8174	14294
V_S	(m/s)	1042	1791	2368
ξ	(%)	3	3	3

3.2 *Mesh Boundaries*

Boundary conditions of the quasi-static model are different from the full-scale models. For a full-scale model, the model side boundaries should be with special energy-absorbing conditions that are set adequately far enough from the structure being analyzed in such a manner that out-going seismic waves be allowed to pass through instead of being trapped and reflected within the model. The quasi-static model boundaries are shown in (Figure 4). Full-scale boundaries are chosen to allow for a wider mesh of about 17 times the size of the tunnel (could reach 300 m width).

3.3 *Model Initial Condition and Construction Sequence*

For the determination of *ΣMStage*, two-dimensional finite element models were calibrated of three-dimensional finite element models with the same model dimensions and configurations.

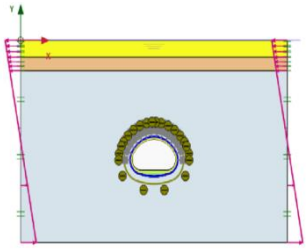

Figure 4. Quasi-static 2D FE model 1 (Q=0.02, D =17.4m).

Examples of meshes used in the two-dimensional and three-dimensional finite element models for Model 1 are shown in (Figures 5 and 6), respectively.

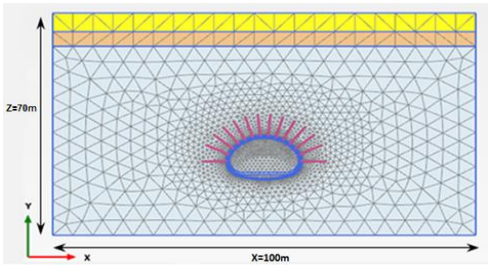

Figure 5. 2-D Finite element model mesh (e.g. Model 1).

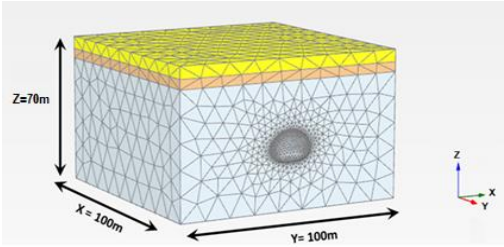

Figure 6. 3-D Finite element model mesh (e.g. Model 1).

Both two- and three-dimensional models have the same construction sequence as shown in (Figures 7 and 8). The calibration was in terms of matching surface, crown settlements, and axial force in the lining.

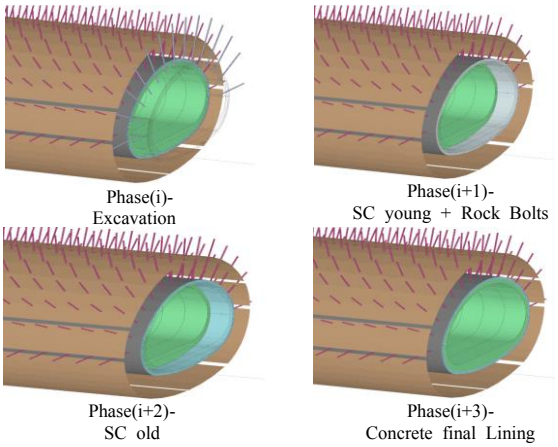

Figure 7. Sequential excavation in 3D model.

The resulted values of stress release obtained from calibration analyses for the 9 models are given in (Table 6) and are applied at the excavation stage of tunneling to account for the stress relaxation in the rock just before initial lining installation.

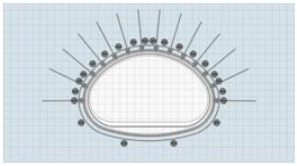

Phase(i)- Excavation (ΣMStage < 1.0)

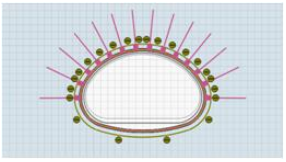

Phase(i+1)-SCyoung+Rock Bolts

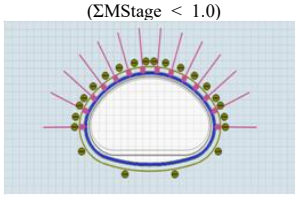

Phase(i+2)-SC old

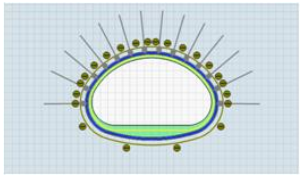

Phase(i+3)-Concrete final Lining

Figure 8. Sequential excavation in 2D model.

Table 6. Rock $\Sigma MStage$ and β for the Models of tunnel sizes 17.4, 10 and 5m in the three rock classes (Q=0.02, 0.4 and 4.0).

Model	Tunnel Size D (m)	Rock Q (--)	ΣMStage (--)	β (--)
Model 1	17.4	0.02	0.386	0.614
Model 2	17.4	0.4	0.124	0.876
Model 3	17.4	4	0.014	0.986
Model 4	10	0.02	0.428	0.572
Model 5	10	0.4	0.138	0.862
Model 6	10	4	0.014	0.986
Model 7	5	0.02	0.372	0.628
Model 8	5	0.4	0.166	0.834
Model 9	5	4	0.028	0.972

4 SEISMIC LOADING AND SEISMIC MODELS

The seismic loading stage is a long term condition at which the final lining is the only rock supporting system while the initial lining is turned off. Three approaches were followed to study the seismic behavior of the proposed 9 models:

- Quasi-static,
- Full-scale seismic modeling of sinusoidal wave, and
- Full-scale seismic modeling of real earthquake records.

4.1 *Presentation of Seismic Load*

For comparison purposes, the same peak ground acceleration (PGA) was used for all three approaches. In this vein, the taken earthquake level is the Maximum Credible EQ (MCE) 2% probability of exceedance for 50 years (Return Period ≈2400ys). The site-specific short-period (Ts=0.2 seconds) spectral acceleration (Ss) equivalent to this level of earthquake is taken from earthquake spectrum records of Turkey and is equal to 1.434 g. By assuming site class A as per (EN 1998-1, 2003) the peak ground acceleration at rigid bedrock (a_{gR}) will be the same as site-specific peak ground acceleration ($a_{max,s}$) and equals 0.574 g.

For quasi-static approach, as per (Pescara et al. 2011) and by using the site-specific peak ground acceleration ($a_{max,s}$) equals 0.574 g, the peak acceleration at tunnel depth is equal to 0.459 g (based on tunnel depth C=0.8) where C is the ratio between the surface wave and the tunnel depth. Peak ground velocity is 0.445m/s as per (Power et al 1996). Accordingly, the maximum shear strain deformation in the free-field condition γ_{max}= 2.22 x 10^{-4} based on apparent propagation S-wave velocity Cs=2000m/s as suggested by (O'Rourke & Liu 1999, Power et al. 1996, Paolucci & Pitilakis 2007). Knowing the model height (about 70m), the horizontal displacement Δx_{max} applied to the model to simulate the shear strain in the quasi-static approach shall equal to 0.156m. All the above results are summarized in (Table 7).

Table 7. Free-field method result used as input for the quasi-static approach numerical model.

Ss Short-period Spectral Acc. (g)	a_{gR} PGA @ rigid bedrock (g)	$a_{max,s}$ Site-specific PGA (g)	$a_{z,max}$ Peak Acc. @ Tunnel Depth (g)	Vs PGV (m/sec)	Cs Apparent S-wave Velocity (m/sec)	γ_{max} Max. Free-field Shear Strain (-)	Δx_{max} Hz. Disp. (m)
1.434	0.57	0.57	0.45	0.445	2000	2.2E-4	0.0156

For full-scale seismic modeling of sinusoidal wave approach, uniform sinusoidal acceleration-time history with frequency 8Hz and peak ground acceleration of 0.574g was proposed (see Figure 9). The value of frequency proposed is selected after a set of parametric studies performed by the Author of this paper (Salem et al. 2020) for the most applicable frequency value for better simulation of an earthquake record.

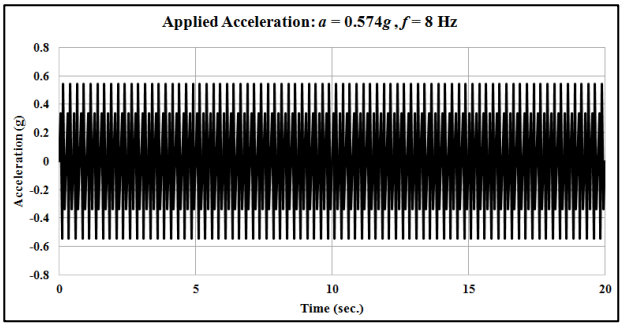

Figure 9. Uniform sinusoidal acceleration–time history with frequency 8.0 Hz with PGA=0.574g.

For full-scale seismic modeling of real earthquake record approach, site-specific earthquake acceleration time history record of Duzce 1999 was selected from Turkey earthquake database and scaled using simple scaling approach to peak ground acceleration of 0.574 g (see Figure 10).

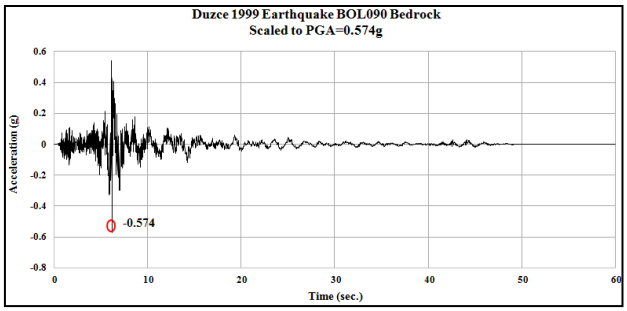

Figure 10. Site-specific bedrock acceleration–time history record of Duzce 1999 earthquake scaled to PGA=0.574g.

5 RESULTS

Axial force and bending moment in the final lining were obtained from the 9 models when subjected to the three seismic loading approaches representing equal seismic loads (quasi-static, Full-scale seismic modeling of a sinusoidal wave with frequency 8Hz, and Full-scale seismic modeling of Duzce 1999 earthquake record). Figure 11 shows axial forces plotted along the tunnel perimeter length for all model cases.

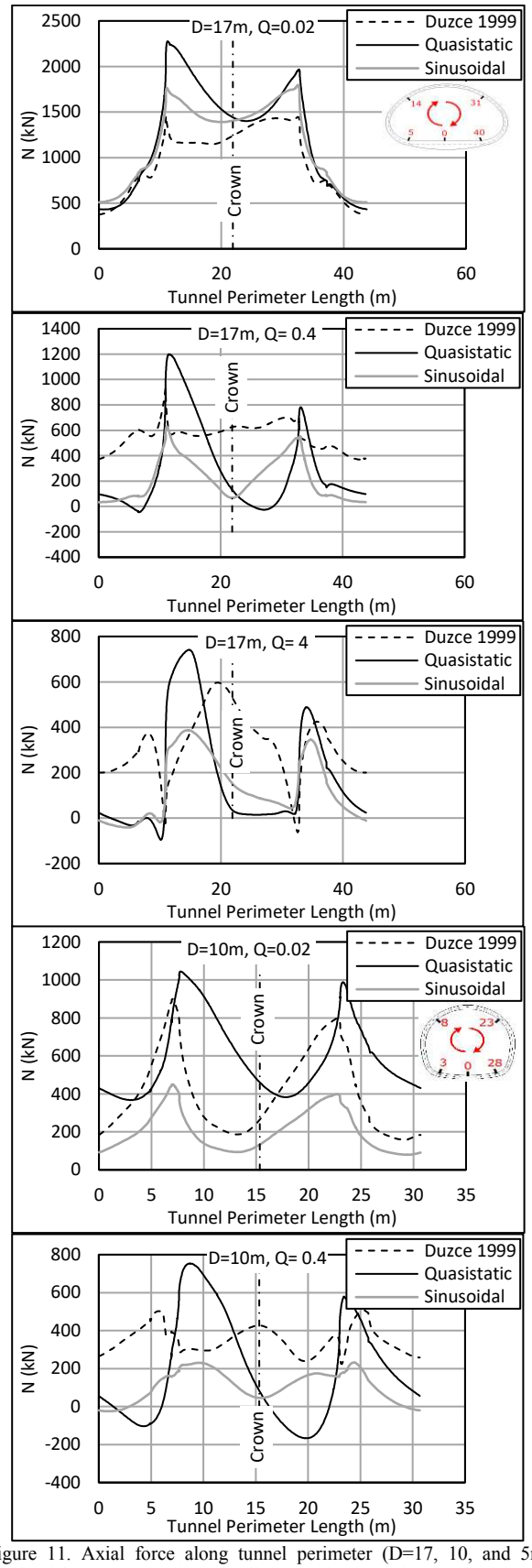

Figure 11. Axial force along tunnel perimeter (D=17, 10, and 5m) obtained from quasi-static and full-scale seismic analyses (Q=0.02, 0.4, and 4.0).

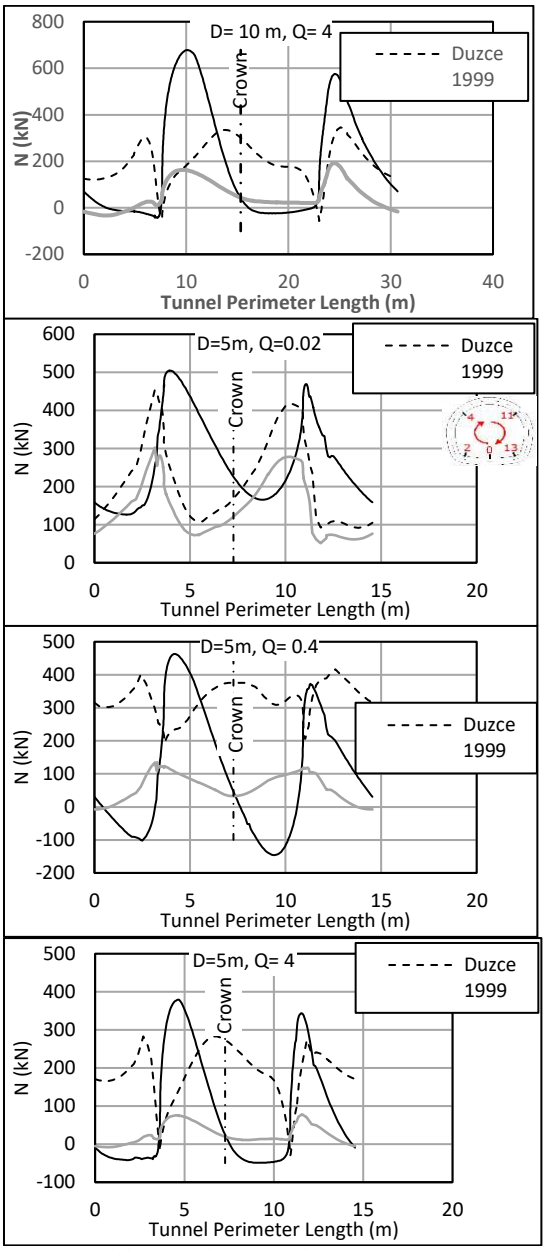

Figure 12. Axial force along tunnel perimeter (D=17, 10, and 5m) obtained from quasi-static and full-scale seismic analyses (Q=0.02, 0.4, and 4.0) [Continued].

From the figures, it can be concluded that maximum seismic normal forces occur near the shoulders of the tunnels. For quasi-static cases, tension values can be developed in the shoulder and opposite sidewall and this is more pronounced in smaller tunnel sizes and higher Q-values. The quasi-static analysis provides slightly higher values of axial forces compared to Duzce 1999 Earthquake regardless of tunnel size and rock Q-value. The average normal force is higher in the Duzce 1999 case as compared to that of the quasi-static case and no tension forces are noticed in this case. Bending moment of the three seismic loading approaches were plotted along the tunnel perimeter length for each model as given in (Figure 12).

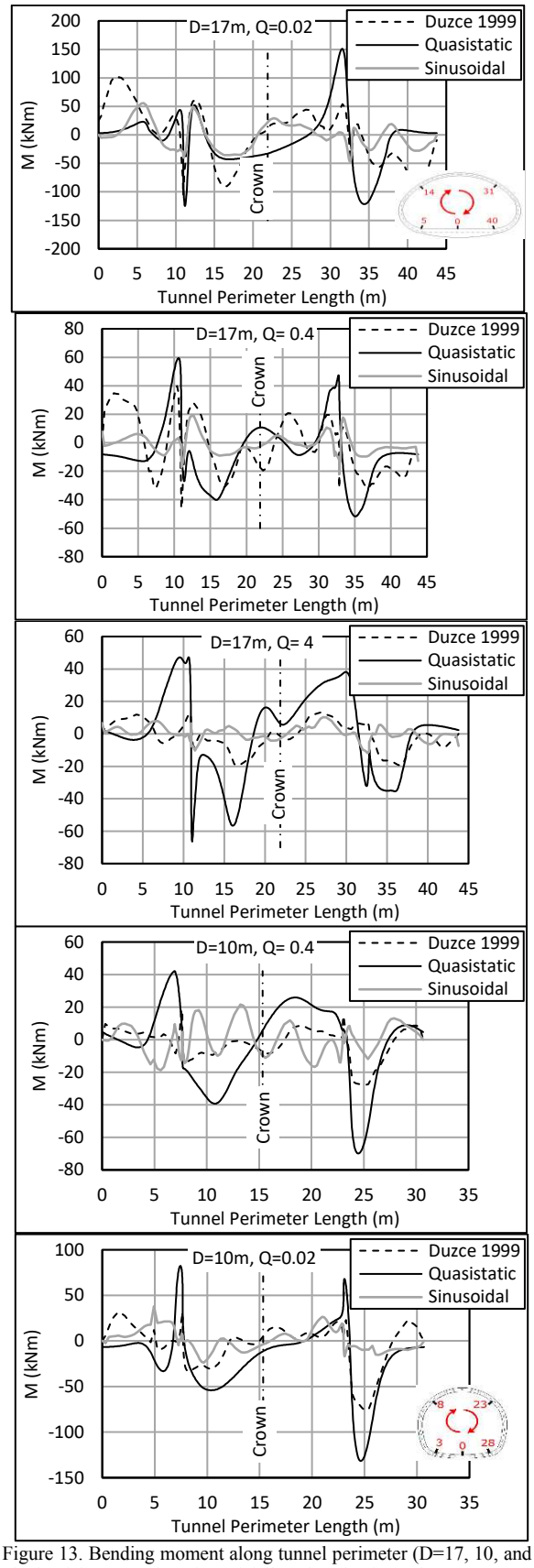

Figure 13. Bending moment along tunnel perimeter (D=17, 10, and 5m) obtained from quasi-static and full-scale seismic analyses (Q=0.02, 0.4, and 4.0).

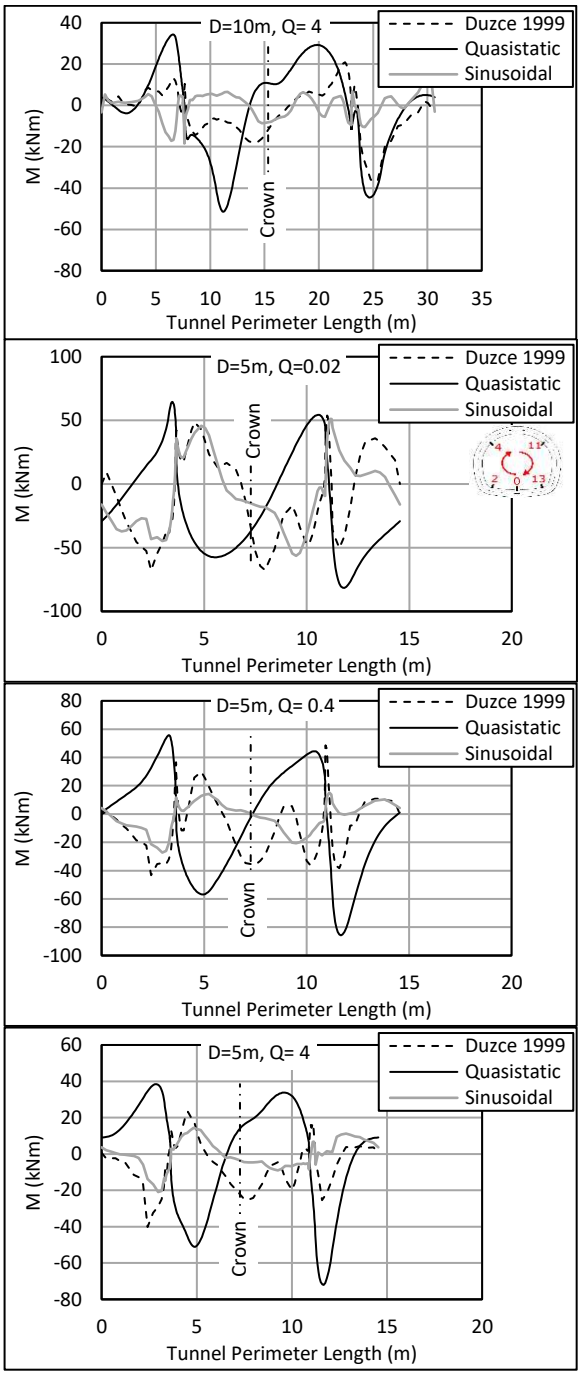

Figure 14. Bending moment along tunnel perimeter (D=17, 10, and 5m) obtained from quasi-static and full-scale seismic analyses (Q=0.02, 0.4, and 4.0) [Continued].

From the figures, the quasi-static analysis provides higher values of bending moments compared to full-scale analyses regardless of tunnel size and rock Q-value.

Example of relative shear stress contours obtained from Model 1 (Q=0.02, D =17.4m) applying quasi-static, full-scale analysis using sinusoidal wave as input motion and full-scale analysis of real earthquake record for are given in Figures 13, 14, and 15, respectively.

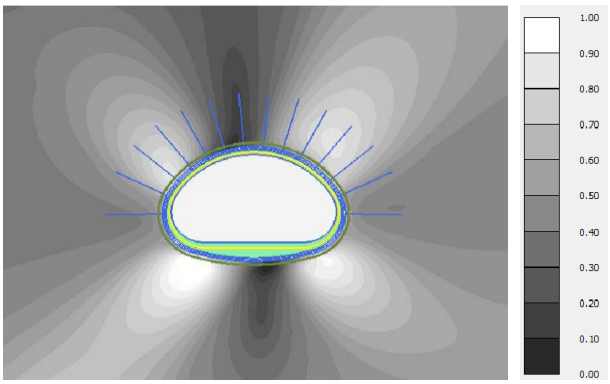

Figure 15. Relative shear stress developed in tunnel (D=17.4) obtained from quasi-static analysis (Q=0.02).

From Figure 13, it can be noticed that quasi-static relative shear stress distribution is close to the typical tunnel shear stress distribution under static loading condition because of its intrinsic static behavior.

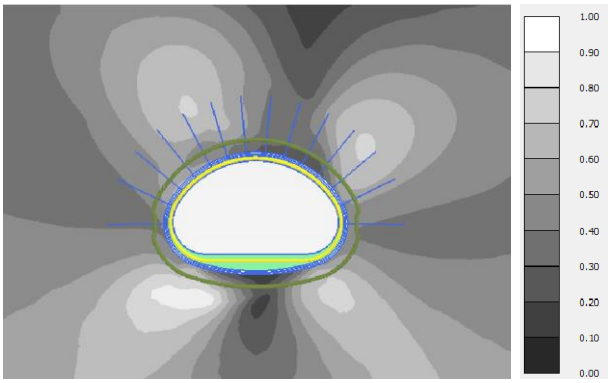

Figure 16. Relative shear stress developed in tunnel (D=17.4) obtained from full-scale sinusoidal (8Hz) analysis (Q=0.02).

From Figure 14, full-scale analysis using sinusoidal wave show relative shear stress distribution close to the quasi-static analysis distribution with a conspicuous concentration of shear stress at quadrant points of the tunnel.

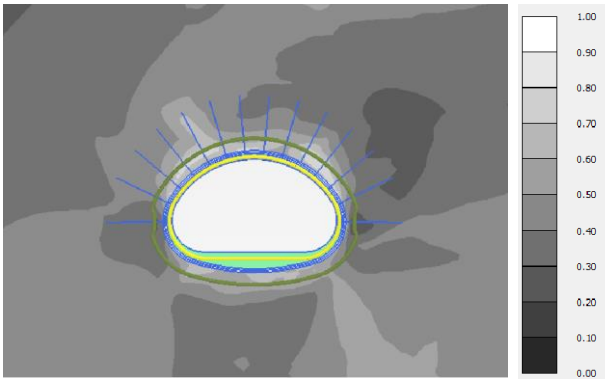

Figure 17. Relative shear stress developed in tunnel (D=17.4) obtained from full-scale seismic (Duzce 1999) analysis (Q=0.02).

From Figure 15, relative shear stress in the case of full-scale analysis of real earthquake record is lower than those of the other two seismic loading models. Maximum values are depicted at the upper half of the tunnel with special concentration at high curvature points.

5 ANALYSIS

Based on results of axial force along tunnel perimeter obtained from different seismic analysis approaches for models 1 to 9, relations between maximum axial force and Q-value of rock for different tunnel sizes (D=17, 10, and 5m) are shown in Figure 16. Similarly, relations between maximum axial force and Tunnel size D and for different Q-values of rock (Q=0.02, 0.4, and 4m) are shown in Figure 17.

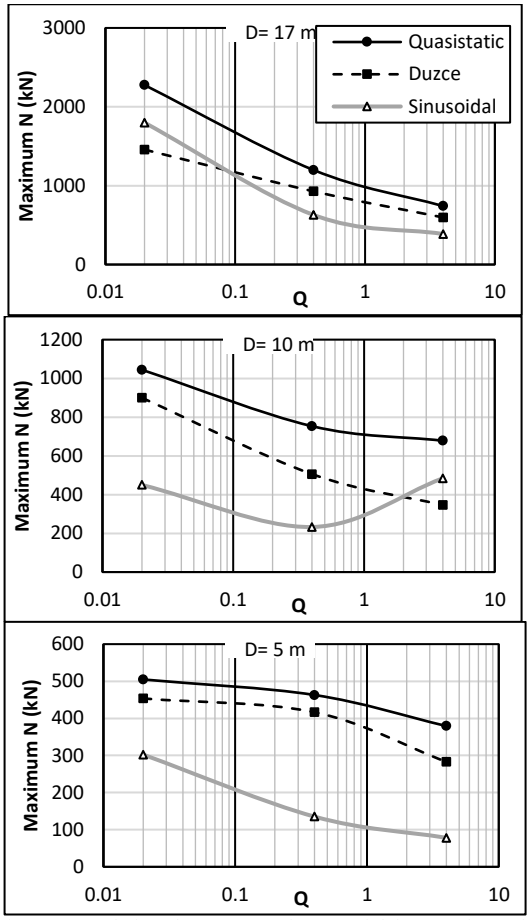

Figure 18. Relations between maximum axial force and Q-value of rock for different tunnel sizes (D=17, 10 and 5m) obtained from quasi-static and full-scale seismic analyses.

From Figure 16, as a general trend, the maximum axial force decreases with increasing the Q-value of rock. Maximum axial force obtained from the Full-scale analysis using sinusoidal waves ranges from 20-80% the maximum axial force obtained from the quasi-static analysis. Maximum axial force obtained from the Full-scale analysis using sinusoidal waves ranges from 50-90% the maximum axial force obtained from the quasi-static analysis.

From Figure 17, as a general trend, the maximum axial force increases with increasing tunnel size D. Quasi-static models give the highest values while sinusoidal models give the lowest values of axial forces. The real earthquake model is noticed to have values in between the other two cases.

Relations between maximum absolute bending moment and Q-value of rock for different tunnel sizes (D=17, 10, and 5m) are shown in Figure 18. Similarly, relations between maximum absolute bending moment and Tunnel size D for different Q-values of rock (Q=0.02, 0.4, and 4m) are shown in Figure 19.

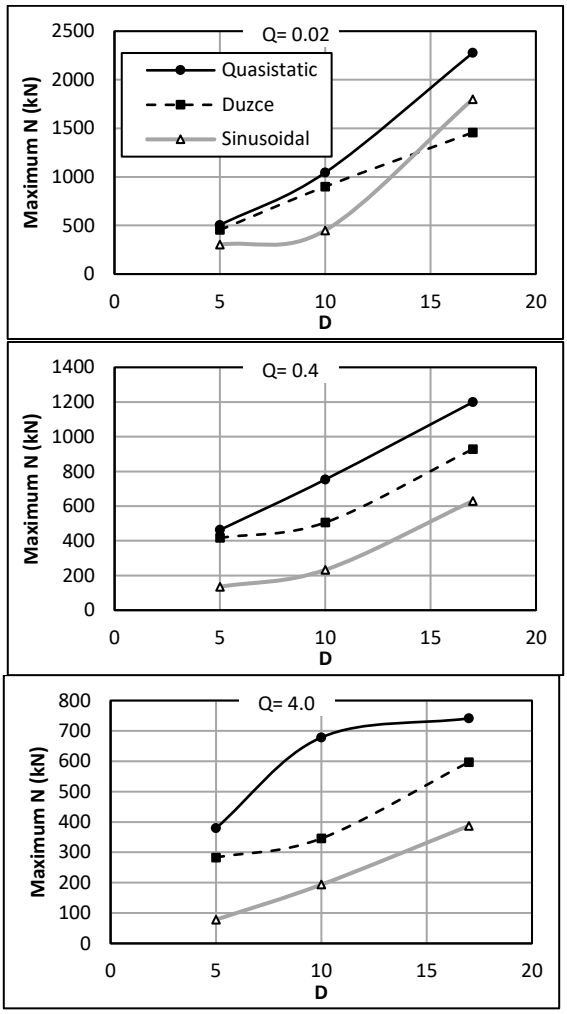

Figure 19. Relations between maximum axial force and tunnel size D for different Q-values of rock (Q=0.02, 0.4, and 4m) obtained from quasi-static and full-scale seismic analyses.

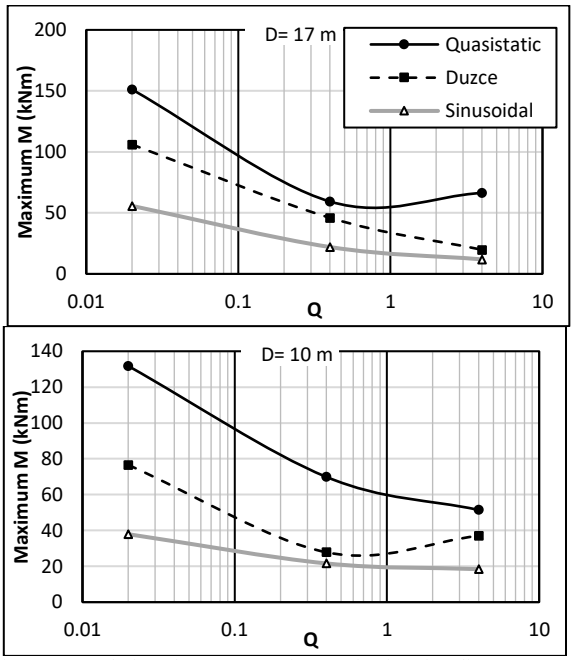

Figure 20. Relations between maximum absolute bending moment and Q-value of rock for different tunnel sizes (D=17, 10, and 5m) obtained from quasi-static and full-scale seismic analyses.

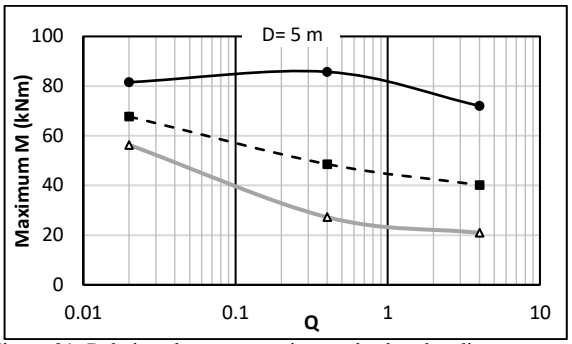

Figure 21. Relations between maximum absolute bending moment and Q-value of rock for different tunnel sizes (D=17, 10, and 5m) obtained from quasi-static and full-scale seismic analyses [Continued].

From Figure 18, as a general trend, the maximum absolute bending moment decreases with increasing the Q-value of rock with the quasi-static case always the highest values. The maximum absolute bending moment obtained from the Full-scale analysis using sinusoidal waves ranges from 20-70% the maximum absolute bending moment obtained from the quasi-static analysis. While the maximum absolute bending moment obtained from the Full-scale analysis using sinusoidal waves ranges from 30-85% the maximum absolute bending moment obtained from the quasi-static analysis.

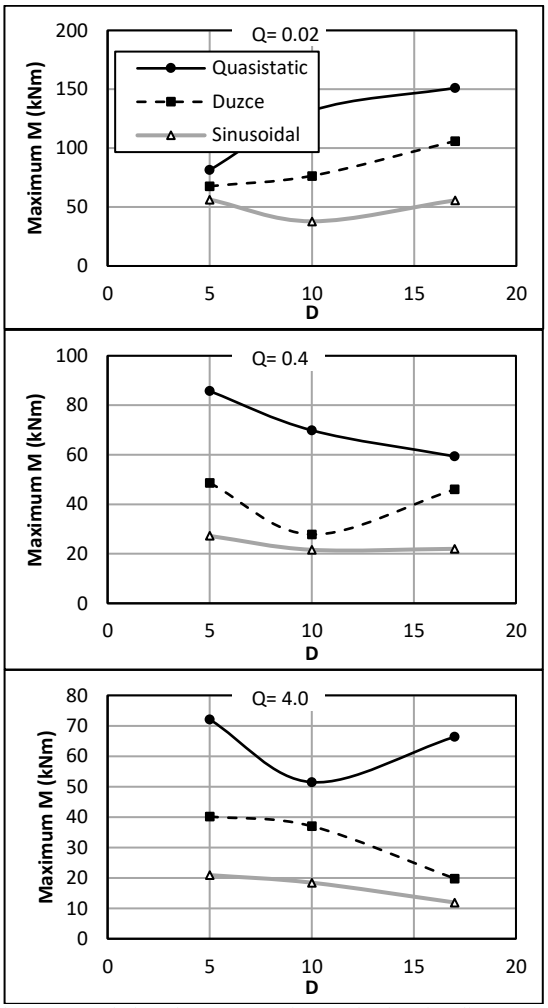

Figure 22. Relations between maximum absolute bending moment and tunnel size D for different Q-values of rock (Q=0.02, 0.4, and 4m) obtained from quasi-static and full-scale seismic analyses.

From Figure 19, tunnel size has no distinct effect on the magnitude of maximum absolute bending moment. Quasi-

static cases are always higher than real earthquake cases and sinusoidal cases give the lowest bending moment values.

Interaction Diagrams of final lining concrete section with compressive strength R_{ck} = 37 MPa and thickness t = 50 cm reinforced with steel reinforcement Y14/15cm are constructed for the case of Q= 0.02 as an example as shown in Figure 20.

From Figure 20, it can be concluded that, although the concrete section is safe in all cases, real earthquake models are relatively closer to the interaction envelope due to lower normal forces and higher bending moments.

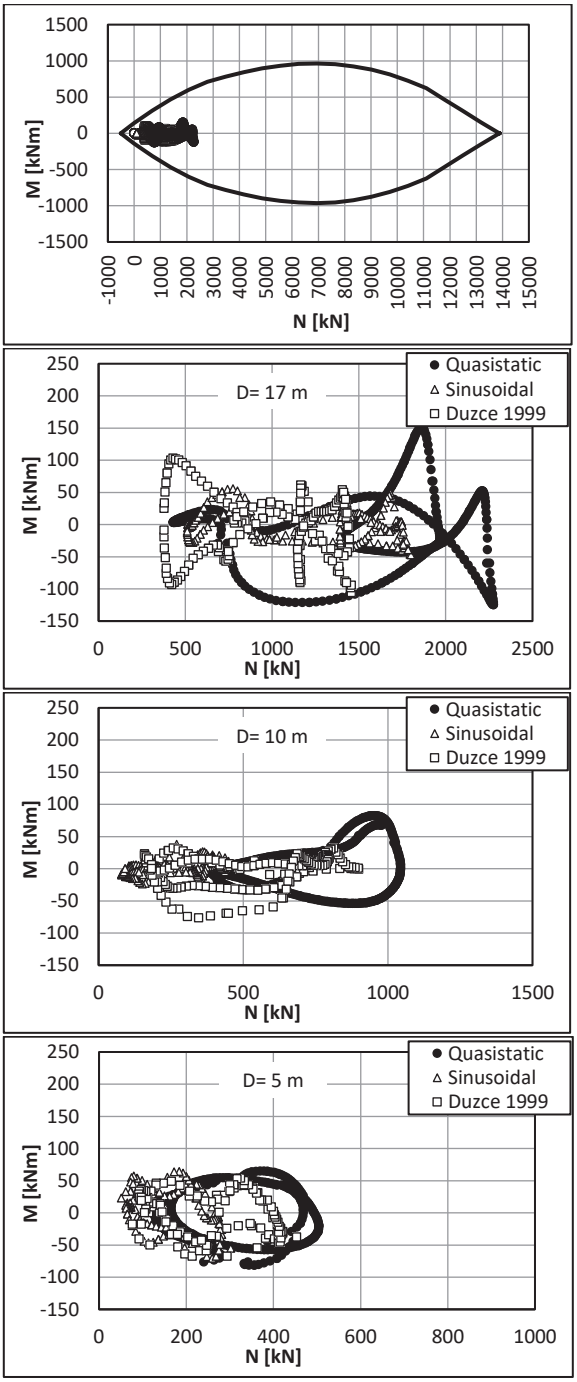

Figure 23. Interaction diagrams for tunnel sizes (D=17.4, 10, 5m) constructed in rock Q=0.02 obtained from quasi-static analysis and full-scale seismic analyses.

6 CONCLUSIONS

A study is conducted to estimate the seismic effect on different tunnel sizes constructed in different rock qualities and subjected to different seismic analysis approaches while maintaining the same seismic load. The following main conclusions can be drawn:

1- Quasi-static analysis approach provides conservative maximum axial force and bending moment compared to full-scale seismic analyses.
2- Full-scale seismic analysis using sinusoidal wave provides the best estimate for preliminary design when no available accurate design earthquake data or seismic hazard assessment study.
3- Maximum axial force as a general trend decrease with increasing Q-value of rock and increase with increasing tunnel size D.
4- Maximum absolute bending moment as a general trend decrease with increasing Q-value of rock.
5- Tunnel size has no distinct effect on the magnitude of maximum absolute bending moment.

7 ACKNOWLEDGEMENTS

This paper is dedicated to the memorial of late Prof. Dr. Sherif Wissa Agaiby: Professor of Soil Mechanics and Foundations, Cairo University, Egypt.

8 REFERENCES

Barton, N., Lien, R., and Lunde, J. (1974). "Engineering classification of rock masses for the design of tunnel support," Rock Mechanics, Vol. 6, No. 4. pp. 189-236.

Barton, N. (2002). "Some new Q-value correlations to assist in site characterisation and tunnel design," International Journal of Rock Mechanics and Mining Sciences, 39(2):185-216.

Bilotta, E., Lanzano, G., Russo, G., Santucci, de Magistris, F., Silvestri, F. (2007c). "Methods for the seismic analysis of transverse section of circular tunnels in soft ground," ISSMGE-ERTC12 Workshop at XIV ECSMGE, Geotechnical Aspects of EC8, Chapter 22, Madrid Spain.

Corigliano, M., Scandella, L., Barla, G., Lai, C.G., Paolucci, R. (2007). "Seismic analysis of deep tunnels in weak rock: a case study in Southern Italy," Proceedings of Fourth International Conference on Earthquake Geotechnical Engineering, June 25-28, Paper No. 1616, Thessaloniki Greece.

EN 1998-1 (2003). "Eurocode 8: Design of structure for earthquake resistance, Part 1: General rules, seismic actions and rules for buildings," CEN European Committee for Standardization, Brussels, Belgium.

Grimstad, E. (2007). "The Norwegian method of tunnelling - a challenge for support design," XIV European Conference on Soil Mechanics and Geotechnical Engineering, Madrid.

Gutenberg, B. (1951). "The elastic constants in the interior of the Earth," Internal Constitution of the Earth, 2d ed., 439 p., New York: Dover, pp. 364-81.

Hashash, Y.M.A., Hook, J.J., Schmidt, B. and Yao, J.I-C. (2001). "Seismic design and analysis of underground structures," Journal of Tunneling and Underground Space Technology, Vol. 16, Elsevier Science Ltd., pp. 247-293.

Hoek, E. and Diederichs, M. S. (2006). "Empirical estimation of rock mass modulus," International Journal of Rock Mechanics and Mining Sciences, 36, pp. 203–215.

Joshi, V. H. and Emery, J. J. (1980). "Seismic response of tunnels," Proc. of the 2nd Int. Conference on Ground Movement and Structures, Wales Institute of Science and Technology, Gardiff, pp. 581-590.

Lanzano, G. (2009). "Physical and Analytical Modeling of Tunnels under Dynamic Loadings," Ph.D. thesis, University of Naples.

Lee, I.M. and An, D. J. (2001). "Seismic analysis of tunnel structures," Korean tunneling association.

NGI (1997). “Engineering Geology-Practical application of the Q-method,” Technical Report 592046-4, Norwegian Geotechnical Institute, Sognsveien 72, N-0806 Oslo.

O’Rourke, M.J. and Liu, X. (1999). “Response of buried pipelines subject to Earthquake effects,” Monograph No.III, MCEER (Multidisciplinary Center for Earthquake Engineering Research) Publications, University at Buffalo, Red Jacket Quadrangle, Buffalo, NY 14261.

Palmstrom, A, Singh, R. (2001). “The deformation modulus of rock masses: comparisons between in situ tests and indirect estimates,” Tunnelling Underground Space Technol 2001;16:115–31.

Paolucci, R., Pitikalis, K. (2007). “Seismic risk assessment of underground structures under transient ground deformation,” In Pitikalis, K. (editor). Earthquake Geotechnical Engineering. Chapter 18, pp 433-459. Springer Vienna.

Penzien, J. (2000). “Seismically-induced racking of tunnel linings,” International Journal of Earthquake Engineering and Structural Dynamics, Vol. 29, pp. 683-691.

Pescara, M., Gaspari, G. M., Repetto, L. (2011). “Design of underground structures under seismic conditions: a long deep tunnel and a metro tunnel,” ETH Zurich, 15 Dec. 2011, Colloquium on seismic design of tunnels, pp. 1-37.

Power, M.S., Rosidi, D., Kaneshiro, J. (1996). “Vol. III Strawman: screening, evaluation, and retrofit design of tunnels,” Report Draft. National Center for Earthquake Engineering Research, Buffalo, New York.

Power, M.S., Rosidi, D., Kaneshiro, J.Y. (1998). “Seismic vulnerability of tunnels and underground structures revisited,” Proceedings of North American Tunneling ’98, Newport Beach, CA, Balkema Rotterdam, pp. 243-250.

Salem A.N., Ezzeldine O.Y., Amer M.I. (2020). “Seismic Analysis of Rock Tunnels,” Ph.D. thesis, Cairo University, Egypt.[In print]

Sarfeld, W., Klapperich, H. and Savidis, S. (1985). “Dynamic interaction between tunnel and surrounding soil due to seismic loading,” Proc. of the 11th Conference on Soil Mechanics and Foundation Engineering, San Francisco, pp. 1873-1876.

Stein, S. and Wysession, M. (2003). “An Introduction to Seismology, Earthquakes, and Earth Structure,” Blackwell Publishing, Oxford, UK.

Wang, J. (1993). “Seismic Design of Tunnels - A Simple State-of-the-art Design Approach,” Monograph 7, Parsons, Brinckerhoff, One Penn Plaza, Quade and Douglas Inc, New York.